

---

# Toward Metrics for Differentiating Out-of-Distribution Sets

---

**Mahdieh Abbasi**  
Université Laval

mahdieh.abbasi.1@ulaval.ca

**Changjian Shui**  
Université Laval

changjian.shui.1@ulaval.ca

**Arezoo Rajabi**  
Oregon State University

rajabia@oregonstate.edu

**Christian Gagné**  
Université Laval

christian.gagne@gel.ulaval.ca

**Rakesh B. Bobba**  
Oregon State University

rakesh.bobba@oregonstate.edu

## Abstract

Vanilla CNNs, as uncalibrated classifiers, suffer from classifying out-of-distribution (OOD) samples nearly as confidently as in-distribution samples, making them indistinguishable from each other. To tackle this challenge, some recent works have demonstrated the gains of leveraging readily accessible OOD sets for training end-to-end calibrated CNNs. However, a critical question remains unanswered in these works: how to select an OOD set, among the available OOD sets, for training such CNNs that induces high detection rates on unseen OOD sets? We address this pivotal question through the use of Augmented-CNN (A-CNN) involving an explicit rejection option. We first provide a formal definition to precisely differentiate OOD sets for the purpose of selection. As using this definition incurs a huge computational cost, we propose novel metrics, as a computationally efficient tool, for characterizing OOD sets in order to select the proper one. In a series of experiments on several image and audio benchmarks, we show that training an A-CNN with an OOD set identified by our metrics (called A-CNN\*) leads to remarkable detection rate of unseen OOD sets while maintaining in-distribution generalization performance, thus demonstrating the viability of our metrics for identifying the proper OOD set. Furthermore, we show that A-CNN\* outperforms state-of-the-art OOD detectors across different benchmarks.

## 1 Introduction

In learning theory, it is assumed that a training set and a held-out test set are drawn independently from the same data distribution, which is called in-distribution set. While this assumption can be true for many restricted laboratory environments, it rarely holds for many real-world applications, where the samples can be drawn from both in-distribution and from out-of-distribution (OOD) data containing novel samples semantically and statistically different from those of in-distribution. In the presence of OOD samples, it is important for a model to distinguish them to make reliable decisions. However, Guo *et al.* [10] have shown that the state-of-the-art (vanilla) deep neural network (e.g. CNN) are uncalibrated such that their predictions for the OOD samples are nearly as confident as that of in-distribution samples, making them indistinguishable from each other. For safety-critical real-world applications such as self-driving cars, using vanilla CNNs that tend to confidently make wrong decisions for such unknown OOD samples can lead to serious safety and security consequences.

To tackle this challenge, many post-processing approaches [11, 15, 16] attempt to process the predictive confidence of pre-trained vanilla CNNs with the aim of creating a gap between the confidence for OOD samples and that of in-distribution ones. However, their performance is dependent

on several additional hyper-parameters such as temperature, amount of additive noise, and threshold on the processed confidence prediction, etc, which all need to be carefully tuned.

More recently, some researchers [3, 12, 17] have moved toward *end-to-end* calibrated CNNs by forcing them directly to provide uncertain predictions for OOD samples while still confidently and correctly classifying in-distribution ones. To train these models, they have leveraged a naturalistic OOD set<sup>1</sup> that is selected *manually* from among many available ones, without providing a systematic basis (or some solid justifications) for their selection. However, a pivotal question remains unanswered: *how to differentiate among OOD sets for selecting a proper one, which in turn induces a well-generalized calibrated model with high detection rate of unseen OOD sets?* Although Hendrycks *et al.* [12] have conjectured a few clues to differentiate them, our main focus is to answer this crucial question concretely.

Instead of making uncertain predictions for OOD samples, with the use of classical idea of adding an explicit rejection option (e.g., [1, 5, 9]), the OOD samples can be directly rejected by classifying them to the extra class. Thus, we exploit Augmented CNNs (A-CNNs), i.e., a vanilla CNN with an extra class augmented to its pre-defined classes, by leveraging OOD set (along with in-distribution set/task) for training it. Interestingly, A-CNN can perform OOD sample detection without introducing any auxiliary hyper-parameters (e.g., threshold on confidence score) by explicitly rejecting them as the extra class. However, without answering the aforementioned question, training an A-CNN is still computationally challenging due to availability of enormous number of OOD sets.

In this paper, we first provide a formal definition for selecting a proper OOD set with the aim of training a well-generalized A-CNN with high detection rate for unseen OOD sets. However, selection of a proper OOD set according to this definition is computationally expensive. To overcome this, we propose some metrics that can be efficiently computed using a vanilla CNN trained on a given in-distribution task. We drive our metrics according to the following intuition: a proper OOD set should cover the in-distribution sub-manifolds which are achieved by the penultimate layer of a vanilla CNN. We call such OOD sets as *protective* OOD sets. Protecting in-distribution sub-manifolds allows for rejecting automatically the unseen OOD sets that are located relatively far away from the in-distribution sub-manifolds, as shown in Figure 1.

Our contributions in this paper can be outlined as follows:

- We provide a formal definition for precisely describing a proper OOD set for training a well-generalized A-CNN, which also leads to high detection rate of OOD sets.
- We are first to propose novel quantitative metrics as a computationally efficient tool for differentiating OOD sets with the aim of selecting a proper (i.e., most protective) OOD set w.r.t. a given in-distribution set. These metrics, namely **Softmax-based Entropy (SE)**, **Coverage Ratio (CR)** and **Coverage Distance (CD)**, can be *efficiently* computed using a vanilla CNN trained on the given in-distribution task.
- Evaluating the proposed metrics for recognizing the most and the least protective OOD set over an extensive range of OOD sets w.r.t. image classification tasks (i.e., SVHN and CIFAR-10) and an audio classification task (i.e., Urban-sound). We verify our metrics for selecting the most protective OOD set, which in turn leads to training A-CNNs with significantly high OOD detection rate while maintaining in-distribution generalization performance.

## 2 Characterizing a Proper OOD Set

### 2.1 Preliminaries

Let’s assume a hypothesis class  $\mathcal{H}'$  for a  $K + 1$  classification problem with  $K$  classes associated for a given in-distribution task and the extra class (i.e.,  $(K + 1)$ -th class) reserved for OOD samples. Moreover,  $\mathcal{S}_I = \{(\mathbf{x}_I^i, \mathbf{y}_I^i)\}_{i=1}^N$  denotes an in-distribution training set consisting of  $N$  i.i.d. labeled samples drawn from data distribution  $\mathcal{D}_I$ , with true label  $\mathbf{y}_I^i \in \{1, \dots, K\}$ . As an OOD training set, take  $\mathcal{S}_O = \{(\mathbf{x}_O^j)\}_{j=1}^M$  involving  $M$  i.i.d. unlabeled samples drawn from a data distribution  $\mathcal{D}_O$ , which we label as  $(K + 1)$ -class.

<sup>1</sup>We simply call OOD set instead of naturalistic OOD throughout the paper.

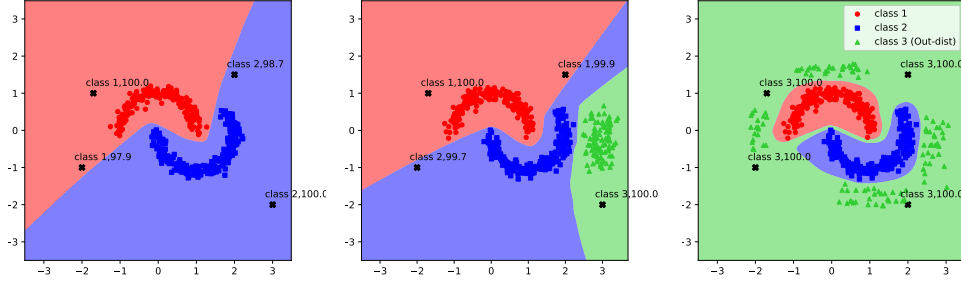


Figure 1: Illustration of properties of a partially-protective OOD set (middle) and a protective one (right) and their effect on training A-MLP for two-moons classification dataset. (left) a vanilla MLP trained on two-moons dataset. The black-cross samples are some test OOD samples and their predicted class and confidence scores by each (A)-MLP are also indicated. All MLPs are made of three layers with ReLU activation function.

The loss of a hypothesis  $h' \in \mathcal{H}'$  for a given in-distribution sample can be defined as  $\ell(h'(\mathbf{x}_I^i), \mathbf{y}_I^i) = \mathbb{I}(h'(\mathbf{x}_I^i) \neq \mathbf{y}_I^i)$  and its loss for an OOD sample is  $\ell(h'(\mathbf{x}_O^j), K + 1) = \mathbb{I}(h'(\mathbf{x}_O^j) \neq K + 1)$ <sup>2</sup>. An augmented classifier  $h' \in \mathcal{H}'$  is evaluated using the following losses:

*Empirical loss* computed on training set  $\mathcal{S}_I$  and  $\mathcal{S}_O$ :

$$L_{\mathcal{S}_I}(h') = \frac{1}{N} \sum_{i=1}^N \ell(h'(\mathbf{x}_I^i), \mathbf{y}_I^i); \quad L_{\mathcal{S}_O}(h') = \frac{1}{M} \sum_{j=1}^M \ell(h'(\mathbf{x}_O^j), K + 1).$$

*True loss* computed on the underlying data distributions  $\mathcal{D}_I$  and  $\mathcal{D}_O$ :

$$L_{\mathcal{D}_I}(h') = \mathbb{E}_{(\mathbf{x}_I, \mathbf{y}_I) \sim \mathcal{D}_I} \ell(h'(\mathbf{x}_I), \mathbf{y}_I); \quad L_{\mathcal{D}_O}(h') = \mathbb{E}_{\mathbf{x}_O \sim \mathcal{D}_O} \ell(h'(\mathbf{x}_O), K + 1).$$

Before presenting our definition, we remark that there is a set of  $B$  “out” data distributions  $\mathcal{D}_O^b$  ( $b = \{1, \dots, B\}$ ) with their respective OOD training set  $\mathcal{S}_O^b \sim \mathcal{D}_O^b$ . Theoretically speaking,  $B$  can be infinitely large. Moreover, we assume generalization error of vanilla classifier (denoted by  $h \in \mathcal{H}$ ), for the original  $K$  classification task, trained on  $\mathcal{S}_I$  is small:  $|L_{\mathcal{S}_I}(h) - L_{\mathcal{D}_I}(h)| \leq \epsilon$ .

**Definition 1** : For a given out-of-distribution training set  $\mathcal{S}_O^b \sim \mathcal{D}_O^b$  and in-distribution training set  $\mathcal{S}_I$  w.r.t. hypothesis class  $\mathcal{H}'$ ,  $\mathcal{D}_I$  and  $B$  “out” data distributions, we define two kinds of gaps for augmented classifier  $h' \in \mathcal{H}'$ :

$$\mathcal{L}_{\mathcal{S}_I} = |L_{\mathcal{S}_I}(h') - L_{\mathcal{D}_I}(h')| \quad (1)$$

$$\mathcal{L}_{\mathcal{S}_O^b} = \sup_{\mathcal{D}_O \in \{\mathcal{D}_O^1, \dots, \mathcal{D}_O^B\}} |L_{\mathcal{S}_O^b}(h') - L_{\mathcal{D}_O}(h')| \quad (2)$$

The first gap,  $\mathcal{L}_{\mathcal{S}_I}$ , represents the gap between empirical loss of classifier  $h' \in \mathcal{H}'$  on in-distribution training set  $\mathcal{S}_I$  and its true loss on  $\mathcal{D}_I$ . Whereas the second gap, i.e.  $\mathcal{L}_{\mathcal{S}_O^b}$  concerns the largest (worst) gap between empirical loss of  $h'$  on OOD training set, i.e.  $\mathcal{S}_O^b$ , and its true loss on “out” data distributions. By restricting  $B$  to a manageable (finite) large number, we re-define  $\mathcal{L}_{\mathcal{S}_O^b}$  by upper-bounding Eq. 2, i.e., sum of gaps on  $B$  finite “out” data distributions:

$$\mathcal{L}_{\mathcal{S}_O^b} = \sum_{\mathcal{D}_O \in \{\mathcal{D}_O^1, \dots, \mathcal{D}_O^B\}} |L_{\mathcal{S}_O^b}(h') - L_{\mathcal{D}_O}(h')|. \quad (3)$$

<sup>2</sup>Indicator function  $\mathbb{I}(p)$  returns 1 if condition  $p$  is true, and 0 otherwise.

As true data distributions are unknown, the aforementioned equations can be empirically computed using validation sets. Then, one can recognize the proper OOD set as follows:

$$S_O^* = \underset{S_O^b \in \{S_O^1, \dots, S_O^B\}}{\operatorname{argmin}} \mathcal{L}_{S_I} + \mathcal{L}_{S_O^b} \quad (4)$$

Training an augmented classifier (i.e.  $h' \in \mathcal{H}'$ ) on  $S_O^*$  (along with  $S_I$ ) leads to small generalization errors on in-distribution task and high detection rate on OOD sets. Unfortunately it is not computationally efficient to use Eq. 4 for finding a proper OOD set as it involves training  $B$  individual classifiers  $h'$ , i.e., train each  $h'$  on a pair of  $(S_I, S_O^b)$ ,  $b \in \{1, \dots, B\}$ . Particularly for the case of CNNs, this incurs a huge computational overhead. To overcome this computational burden, we devise three metrics, which can be efficiently computed by a vanilla CNN trained on only in-distribution set, with the aim of selecting a proper OOD set.

## 2.2 Proposed Metrics

**Illustrative Example** To give a high-level intuitive explanation of our proposed metrics for recognizing a proper OOD set, we use an example based on the two-moons dataset (as in-distribution task), where each moon is considered as a sub-manifold. Fig. 1(a) exhibits the challenge of OOD samples for a vanilla MLP, which is trained on only in-distribution samples. As can be seen, this vanilla MLP *confidently* classifies OOD samples (indicated with black-crosses) as either “class 1” or “class 2” albeit they clearly belong to *none* of the in-distribution manifolds. In Fig. 1(b) we demonstrate a *partially-protective* OOD set whose samples are almost collapsed and only partially cover one of the sub-manifolds (i.e., the manifold with blue squares). An augmented MLP (A-MLP) trained on two-moons dataset along with this OOD set leads to a classifier with a limited OOD detection performance. More precisely, OOD samples, e.g., the *unseen* black-cross samples, which are laying around *uncovered* parts of the manifolds, are still confidently misclassified by the underlying A-MLP. Whereas, in Fig 1 (c) a proper *protective* OOD set whose samples better cover the in-distribution’s sub-manifolds (two-moons) is shown. As can be seen, training an A-MLP on such protective OOD set (along with in-distribution samples) leads to classifying *unseen* black cross OOD samples as class 3 (i.e., the extra class) as well as classifying automatically the regions out of the manifolds as class 3. This results in an A-MLP with high detection performance on unseen OOD sets (i.e., making the gap in Eq. 2 small). Therefore, the design of our metrics is driven according to this intuition that a proper OOD set should be more protective of (i.e., closely covers) all in-distribution sub-manifolds in the feature space. A similar intuition has been previously exploited by some researchers, e.g., [14, 25], with the aim of only generating synthetic OOD samples.

Note that like other researchers [6, 13], we consider the penultimate layer of a vanilla CNN as a function that transfers samples from high-dimensional input space into a low-dimensional feature space, placing them on data (sub-)manifold(s) [2, 4]. Furthermore, we assume that for a standard multi-classification problem (with  $K$  classes), each class has its own sub-manifold in the feature space where its associated in-distribution samples lie. In the following, we propose our metrics to assess which of the available OOD sets has a better and closer coverage of the sub-manifolds.

### 2.2.1 Softmax-based Entropy

We propose our first metric, namely Softmax-based Entropy (SE), to ensure the samples of a given OOD set are distributed evenly to all sub-manifolds (of a given in-distribution task) such that they have the chance of being covered by these OOD samples. For example, an OOD set, whose samples are misclassified by a given vanilla CNN into *only* a few of in-distribution classes (manifolds) instead of all of them, is deemed as non-protective OOD set. This is because the sub-manifolds, which have no OOD samples being misclassified to them, are still uncovered (e.g., Fig. 1 (b)), thus training A-CNN on such non-protective (or partially-protective) OOD set may lead to limited detection performance of unseen OOD sets. In contrast, the samples of a protective set are expected to be misclassified evenly to all the sub-manifolds, giving them a better chance of being covered.

To quantitatively measure this incidence for a given OOD set w.r.t. an in-distribution set and a vanilla CNN trained on it, we introduce Softmax-based Entropy (SE). First we define  $p(c = k|S_O)$  as the

conditional probability of  $k$ -th class given  $\mathcal{S}_O$  as follows:

$$p(c = k|\mathcal{S}_O) = \frac{1}{M} \sum_{j=1}^M \mathbb{I}_k \left( \operatorname{argmax}(h(\mathbf{x}_O^j)) = k \right), \quad (5)$$

where  $h$  is softmax output of the vanilla CNN trained on  $\mathcal{S}_I$  and  $\mathbb{I}_k(\cdot)$  is an indicator function for  $k$ -th class. It returns 1 if a given OOD sample  $\mathbf{x}_O^j \in \mathcal{S}_O$  is (mis)classified as class  $k$  by  $h$ , otherwise it returns 0. Finally, SE is defined for an OOD set  $\mathcal{S}_O$  as follows:

$$\mathbf{H}(\mathcal{S}_O) = - \sum_{k=1}^K p(c = k|\mathcal{S}_O) \log p(c = k|\mathcal{S}_O). \quad (6)$$

$\mathbf{H}(\mathcal{S}_O)$  shall reflect how uniformly the samples of  $\mathcal{S}_O$  are distributed to in-distribution sub-manifolds (i.e., corresponding to each in-distribution class). Thus, the highest  $\mathbf{H}(\mathcal{S}_O)$  indicates that all the sub-manifolds have (nearly) equal number of OOD samples, whereas the smallest value of  $\mathbf{H}(\mathcal{S}_O)$  indicates some sub-manifolds have a few (or no) OOD samples i.e.,  $\mathbf{x}_O^j \in \mathcal{S}_O$  covering them. That is, a protective OOD set should have higher SE than non-protective ones.

### 2.2.2 Coverage Ratio

Although an OOD set with the high(est) SE confirms OOD samples are evenly distributed to all the sub-manifolds, using solely SE is not sufficient to assure the coverage of these sub-manifolds. Putting differently, an OOD set with the highest SE might still be collapsed and only partially cover some parts of the sub-manifolds. Inspired by covering number notion [22], we introduce our second metric, named coverage ratio (CR), in order to measure coverage of the sub-manifolds. Recall the sub-manifolds are approximated using training in-distribution set in the feature space that is achieved by the penultimate layer of  $h$ . We denote  $\mathbf{z}_I^i$  and  $\mathbf{z}_O^j$  as the representations of  $\mathbf{x}_I^i \in \mathcal{S}_I$  and  $\mathbf{x}_O^j \in \mathcal{S}_O$  in the feature space, respectively.

To formally describe Coverage Ratio (CR), we form a rectangular weighted adjacency matrix  $W \in \mathbb{R}^{N \times M}$  for a given pair  $(\mathcal{S}_I, \mathcal{S}_O)$  with  $N$  in-distribution and  $M$  OOD samples, respectively.  $W_{i,j} = \|\mathbf{z}_I^i - \mathbf{z}_O^j\|_2$  is the distance ( $l_2$ -norm) between in-distribution sample  $\mathbf{z}_I^i$  and OOD sample  $\mathbf{z}_O^j$  in the feature space. The distance between a pair of  $(\mathbf{z}_I^i, \mathbf{z}_O^j)$  is computed only if  $\mathbf{z}_I^i$  is among  $k$ -nearest in-distribution neighbors of  $\mathbf{z}_O^j$ , otherwise  $W_{i,j} = 0$ :

$$W_{i,j} = \begin{cases} \|\mathbf{z}_I^i - \mathbf{z}_O^j\|_2 & \text{if } \mathbf{z}_I^i \in \text{k-NN}(\mathbf{z}_O^j, \mathcal{S}_I) \\ 0 & \text{otherwise.} \end{cases} \quad (7)$$

In other words, for each sample  $\mathbf{z}_O^j$ , we find its  $k$  nearest neighbors from the in-distribution set  $\mathcal{S}_I$  in the feature space. Then if the given  $\mathbf{z}_I^i$  belongs to  $k$ -nearest in-distribution neighbors of  $\mathbf{z}_O^j$ , we set  $W_{i,j}$  to their distance. From matrix  $W$ , we derive a binary adjacency matrix  $A$  as follows;  $A_{i,j} = \mathbb{I}(W_{i,j} > 0)$ . Now using matrix  $A$ , we define CR metric as follows:

$$\mathbf{R}(\mathcal{S}_I, \mathcal{S}_O) = \frac{1}{N} \sum_{i=1}^N \mathbb{I} \left( \sum_{j=1}^M (A_{i,j}) > 0 \right), \quad (8)$$

where  $\mathbb{I}(\sum_{j=1}^M (A_{i,j}) > 0)$  assess whether  $i$ -th in-distribution sample  $\mathbf{x}_I^i$  appears at least one time among the  $k$ -nearest neighbors of  $j$ -th OOD sample  $\mathbf{x}_O^j$  in the feature space. Basically, this metric measures how many in-distribution samples (percentage) are covered by at least one OOD samples from  $\mathcal{S}_O$  in the feature space. Finally, **we estimate an OOD set w.r.t. a given in-distribution set is protective if it has both high SE and high CR.**

It is important to note that SE and CR are complementary. As mentioned earlier, high SE of an OOD set without considering its CR is not sufficient for estimating the protective level of an OOD set. Similarly, from high CR alone without having high SE, an OOD set cannot be considered as protective. This is because, an OOD set with high CR but low SE is not distributed enough among all sub-manifolds and might cover a large portion of only a few sub-manifolds.

### 2.2.3 Coverage Distance

Furthermore, to measure the distance between OOD set  $\mathcal{S}_O$  and the in-distribution data sub-manifolds, the following distance metric, named Coverage Distance (CD), can be driven:

$$D(\mathcal{S}_I, \mathcal{S}_O) = \frac{\sum_{i,j} W_{ij}}{\sum_{i,j} A_{ij}} = \frac{1}{kM} \sum_{i,j} W_{ij}. \tag{9}$$

$D(\mathcal{S}_I, \mathcal{S}_O)$  shows average distance between OOD samples of  $\mathcal{S}_O$  and their  $k$  nearest neighbors from in-distribution set. Note between two OOD sets with the same level of high SE and high CR, the one with smaller CD, which indicates its samples are located nearer to the sub-manifolds, is preferable.

## 3 Experimentation

We conduct a series of experiments on several classification tasks including two image benchmarks namely CIFAR-10 and SVHN and one audio benchmark, namely Urban-Sound [21]. In our experiments, we utilize VGG-16 and a CNN described in [20] for image and audio benchmarks, respectively (see supplementary for details).

Like in [16], for each of these in-distribution task, various naturalistic OOD sets are considered; for image classification tasks, i.e., CIFAR-10 and SVHN, we regard LSUN, ISUN, CIFAR-100 and TinyImageNet as OOD sets and Gaussian noise as a synthetic OOD set. For audio classification task with 10 classes, i.e., Urban-Sound, OOD sets considered are TuT [18], Google Command [24] and ECS (Environmental Sound Classification) [19], as well as white-noise sound as a synthetic OOD set (see supplementary for details).

As A-CNNs have an explicit rejection option (used to explicitly classify OOD samples to the extra class), we consider three criteria to assess **A-CNN performance on in-distribution test set**; (I) Accuracy rate (Acc.)  $\uparrow$ : rate of samples classified correctly as their true associated label ( $\uparrow$  indicates higher is better), (II) Rejection rate (Rej.)  $\downarrow$ : rate of samples misclassified as dustbin ( $\downarrow$  indicates lower is better), (III) Error rate (Err.)  $\downarrow$ : rate of samples that are neither correctly classified nor rejected (Err. rate = 1 - (Acc. rate + Rej. rate)). **A-CNN performance on OOD sets** is evaluated by (I) Rejection rate (Rej.)  $\uparrow$ : percentage (rate) of OOD samples classified as dustbin, and (II) Error rate (Err.)  $\downarrow$ : rate of OOD samples not classified as dustbin (Err. = 1 - Rej.)

Recall that for OOD rejection (detection), we *are not using any threshold on the predictive confidence of A-CNN since it is trained to explicitly classifying OOD samples as the extra class*. Therefore, there are no AUROC and AUPR values as these are computed by varying the threshold. Note, A-CNN’s OOD rejection rate and its in-distribution rejection rate are the same concepts as TNR (True Negative Rate) and FNR (False Negative Rate), respectively.

### 3.1 Assessment of Proposed Metrics

First, to obtain in-distribution sub-manifolds, if in-distribution training set has more than 10,000 samples, we randomly selected 10,000 samples from it, otherwise, we used the whole in-distribution training set. Secondly, we pass the samples through the penultimate layer of a pre-trained vanilla CNN to map them into the feature space. The same procedure is done for the samples of an OOD set to transfer them to the feature space. To fairly compare OOD sets according to their SE and CR values, we also randomly select equal number of OOD samples (10,000 samples) from each OOD set. For OOD sets with various sizes, we take the minimum size for making equal size OOD sets by randomly selecting from them. To compute CR and CD metrics, we set our only hyper-parameter (nearest neighbors considered)  $k = 4$  for all our experiments.

In second column of Table 1, we demonstrate the difference between OOD sets according to their SE, CR, and CD, in order to identify the most and least protective OOD set. Recall that the most protective OOD set should have higher CR and higher SE whereas the least protective one has much lower CR and SE among the available OOD sets. For SVHN task, for example, ISUN, among naturalist OOD sets, and Gaussian noise, as synthetic OOD set, are identified as the least protective sets. Note that despite to high CR of Gaussian noise, its SE is far small, thus causing it to be identified as the least protective. The most protective OOD set for SVHN is CIFAR-100 (i.e., C100) with the highest SE

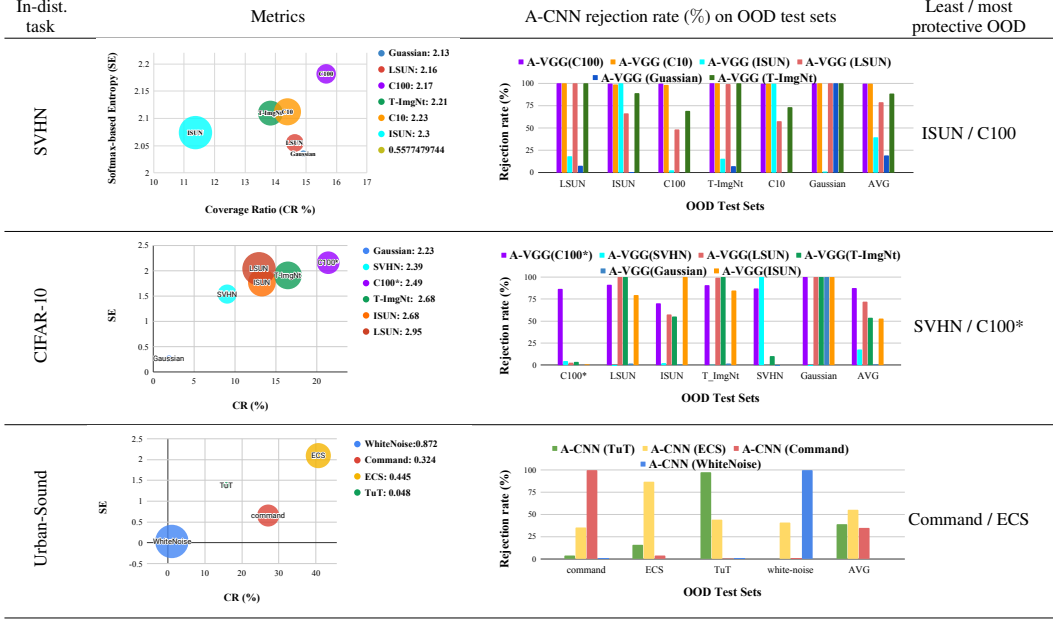


Table 1: Differentiating OOD sets for SVHN, CIFAR-10, and Urban-Sound for purpose of selecting the most protective one using our proposed metrics (SE, CR, and CD). Each figure in 2nd column shows a bubble chart with SE and CR as y-axis and x-axis, respectively. The size of bubbles is determined by CD, also shown in legend of the sub-figures. Third column represents rejection rates of A-CNNs on different OOD sets (x-axis), where each A-CNN is trained on a single OOD set, e.g., A-VGG(C100) trained on CIFAR-100 as OOD set. Last column summarizes the most and the least protective OOD set for each in-distribution task recognized by our metrics (in first columns).

In-dist. task	Network	In-distribution Acc ( $\uparrow$ ) / Rej ( $\downarrow$ ) / Err ( $\downarrow$ )	OOD sets Avg OOD Rej. ( $\uparrow$ )
SVHN	Vanilla VGG	<b>95.53</b> / - / 4.47	-
	A-VGG $^{\ddagger}$ (ISUN)	95.11 / 0 / 4.89	47.23
	A-VGG* (C100)	95.38 / 0.34 / <b>4.28</b>	<b>99.88</b>
CIFAR-10	Vanilla VGG	<b>88.04</b> / - / 11.95	-
	A-VGG $^{\ddagger}$ (SVHN)	87.75 / 0.03 / 12.22	21.41
	A-VGG* (C100*)	85.37 / 5.65 / <b>8.97</b>	<b>85.10</b>
Urban-Sound	Vanilla CNN	<b>67.27</b> / - / 32.73	-
	A-CNN $^{\ddagger}$ (Command)	65.05 / 2.02 / 32.93	26.07
	A-CNN* (ECS)	63.13 / 12.02 / <b>24.85</b>	<b>55.40</b>

Table 2: The influence of selecting the most and the least protective OOD sets on the ability of A-CNNs for detecting unseen OOD sets.

and CR. In the 4th column of Table 1, the most and least protective OOD sets, for each in-distribution task, identified using our metrics are shown.

As we stated in Eq. 4, training an A-CNN on a proper OOD set should lead to a low average (instead of summation, we take average) error rates on unseen OOD sets (or equivalently high average of OOD sample rejection rates). Therefore, for a given in-distribution task (e.g. SVHN), we train A-CNNs on each OOD sets, then evaluate them on all of OOD sets in order to verify the viability of our metrics for selecting a proper OOD set (see third column of Table 1). Evidently, A-CNNs trained on the most protective set (identified by our metrics) across various in-distribution tasks consistently outperform the A-CNNs trained on other OOD sets, particularly the A-CNN trained on the least protective one. For instance, A-CNN trained for SVHN with CIFAR-100 as OOD set has close to 100% rejection rate for all OOD test sets (purple bar in top figure of 3rd column in Table 1). Thus, this shows that *the least protective OOD sets are not completely able to shield the in-distribution sub-manifolds as well as the most protective one. Further, recognizing the most protective OOD set using our metrics is more efficient than doing an exhaustive search over all OOD sets (using Eq. 4).*

It is also interesting to note that even though one may expect Gaussian noise (i.e. white noise) to have well distributed samples, SE metric shows that its samples are actually not evenly distributed

In-dist. Task	Methods	In-dis Rej. (FNR) $\downarrow$ / Avg OOD Rej. (TNR) $\uparrow$
SVHN	Baseline	4.06 / 58.07
	ODIN	4.71 / 69.34
	Mahalanobis Detector	6.40 / 97.41
	A-VGG*	<b>0.34 / 99.88</b>
CIFAR-10	Baseline	7.01 / 44.81
	ODIN	5.81 / 65.74
	Mahalanobis Detector	5.90 / 80.68
	A-VGG*	<b>5.65 / 85.10</b>
Urban-Sound	Baseline	22.83 / 40.96
	ODIN	27.38 / 47.45
	Mahalanobis Detector	16.13 / 45.42
	A-CNN*	<b>12.02 / 55.40</b>

Table 3: Comparison of A-CNN\* with state-of-the-art approaches according to average rejection rates (TNR) of OOD sets and in-distribution rejection rate (FNR). Details are given in the supplementary.

over all of the in-distributed sub-manifolds (having lowest SE) and sometimes (for CIFAR-10 and Urban-Sound in-distribution sets) they even have small coverage rate. As a result, an A-CNN trained on Gaussian noise as OOD set has the lowest average OOD rejection rate.

Furthermore, *in-distribution* generalization performance of two A-CNNs, one trained on the most protective OOD set (named A-CNN\*) and another trained on the least protective one (named A-CNN $\ddagger$ ), are compared with their standard (Vanilla) CNN in Table 2. Although the accuracy rates of the A-CNNs\* drop slightly, their error rates (i.e., risks) are considerably smaller than their counterparts, i.e., vanilla CNNs. This is because the A-CNNs are able to reject some “hard” in-distribution samples, instead of incorrectly classifying them (similar to [7]). For security and safety critical applications such as medical diagnostic systems and self-driving cars it may be better to reject a sample rather than to incorrectly classify it. Moreover, Table 2 shows a significant gap between OOD detection performance of A-CNNs\* and A-CNNs $\ddagger$ , as seen from their average rejection rates on OOD sets. Note that for vanilla CNN the OOD rejection rate is 0 by definition.

### 3.2 Comparison with Related Works

We compare A-CNN\* with three state-of-the-art methods, including baseline [11], ODIN [16], and Mahalanobis-distance-based detector [15] (briefly called Mahalanobis detector)<sup>3</sup>. These approaches attempt to detect OOD samples according to a specific threshold on the modified calibrated predictive confidence scores. As mentioned earlier, TNR and FNR of these methods are the same concept as OOD rejection rate and in-distribution rejection rate, respectively. To set hyper-parameters of these baselines, we use two validation sets with 1000 samples each, for in-distribution and each OOD set. Particularly, for each OOD set using its validation set (along with in-distribution validation set), we set a threshold such that it induces 95% TPR. Then, using these tuned hyper-parameters, we perform OOD detection process on test OOD set and test in-distribution set, reporting TNR and FNR, respectively. As shown in Table 3, A-CNN\* performs *significantly* better than previous works when comparing average OOD rejection and in-distribution rejection rates.

## 4 Conclusion

Our main goal is to differentiate OOD sets for recognizing a proper one for training an end-to-end augmented CNN with high detection rate on unseen OOD sets while maintaining in-distribution generalization performance. To this end, we feature an OOD set as protective if it can cover all of the in-distribution’s sub-manifolds in the feature space. Then, we propose computationally efficient metrics as a tool for differentiating OOD sets for the purpose of selecting the most protective one. In practice, considering the increasing availability of new large-scale datasets for different applications, it is essential to have a tool for efficiently leveraging them for detecting unknown (OOD) samples.

## References

- [1] A. Bendale and T. E. Boult. Towards open set deep networks. In *Proceedings of the IEEE Conference on Computer Vision and Pattern Recognition*, pages 1563–1572, 2016.
- [2] Y. Bengio. Deep learning of representations: Looking forward. In *Statistical language and speech processing*, pages 1–37. Springer, 2013.

<sup>3</sup>We use publicly-available Github codes of the state-of-the-art OOD detectors.



- [3] P. Bevandić, I. Krešo, M. Oršić, and S. Šegvić. Discriminative out-of-distribution detection for semantic segmentation. *arXiv preprint arXiv:1808.07703*, 2018.
- [4] P. P. Brahma, D. Wu, and Y. She. Why deep learning works: A manifold disentanglement perspective. *IEEE transactions on neural networks and learning systems*, 27(10):1997–2008, 2015.
- [5] Q. Da, Y. Yu, and Z.-H. Zhou. Learning with augmented class by exploiting unlabeled data. In *Twenty-Eighth AAAI Conference on Artificial Intelligence*, 2014.
- [6] R. Feinman, R. R. Curtin, S. Shintre, and A. B. Gardner. Detecting adversarial samples from artifacts. *arXiv preprint arXiv:1703.00410*, 2017.
- [7] Y. Geifman and R. El-Yaniv. Selectivenet: A deep neural network with an integrated reject option. *International Conference on Machine Learning (ICML)*, 2019.
- [8] I. J. Goodfellow, J. Shlens, and C. Szegedy. Explaining and harnessing adversarial examples. *International Conference on Learning Representations*, 2015.
- [9] M. Gunther, S. Cruz, E. M. Rudd, and T. E. Boulton. Toward open-set face recognition. In *Proceedings of the IEEE Conference on Computer Vision and Pattern Recognition Workshops*, pages 71–80, 2017.
- [10] C. Guo, G. Pleiss, Y. Sun, and K. Q. Weinberger. On calibration of modern neural networks. In *Proceedings of the 34th International Conference on Machine Learning-Volume 70*, pages 1321–1330. JMLR. org, 2017.
- [11] D. Hendrycks and K. Gimpel. A baseline for detecting misclassified and out-of-distribution examples in neural networks. *arXiv preprint arXiv:1610.02136*, 2016.
- [12] D. Hendrycks, M. Mazeika, and T. G. Dietterich. Deep anomaly detection with outlier exposure. *International Conference on Representation Learning (ICLR)*, 2019.
- [13] F. J. Huang and Y. LeCun. Large-scale learning with svm and convolutional for generic object categorization. In *Computer Vision and Pattern Recognition, 2006 IEEE Computer Society Conference on*, volume 1, pages 284–291. IEEE, 2006.
- [14] K. Lee, H. Lee, K. Lee, and J. Shin. Training confidence-calibrated classifiers for detecting out-of-distribution samples. *arXiv preprint arXiv:1711.09325*, 2017.
- [15] K. Lee, K. Lee, H. Lee, and J. Shin. A simple unified framework for detecting out-of-distribution samples and adversarial attacks. In *Advances in Neural Information Processing Systems*, pages 7167–7177, 2018.
- [16] S. Liang, Y. Li, and R. Srikant. Principled detection of out-of-distribution examples in neural networks. *International Conference on Learning Representation*, 2018.
- [17] M. Masana, I. Ruiz, J. Serrat, J. van de Weijer, and A. M. Lopez. Metric learning for novelty and anomaly detection. *British Machine Vision Conference*, 2018.
- [18] A. Mesaros, T. Heittola, and T. Virtanen. TUT database for acoustic scene classification and sound event detection. In *24th European Signal Processing Conference 2016 (EUSIPCO 2016)*, Budapest, Hungary, 2016.
- [19] K. J. Piczak. Esc: Dataset for environmental sound classification. In *Proceedings of the 23rd Annual ACM Conference on Multimedia*, pages 1015–1018. ACM Press, 2015.
- [20] J. Salamon and J. P. Bello. Deep convolutional neural networks and data augmentation for environmental sound classification. *IEEE Signal Processing Letters*, 24(3):279–283, 2017.
- [21] J. Salamon, C. Jacoby, and J. P. Bello. A dataset and taxonomy for urban sound research. In *Proceedings of the 22nd ACM international conference on Multimedia*, pages 1041–1044. ACM, 2014.
- [22] S. Shalev-Shwartz and S. Ben-David. *Understanding machine learning: From theory to algorithms*. Cambridge university press, 2014.
- [23] F. Tramèr, N. Papernot, I. Goodfellow, D. Boneh, and P. McDaniel. The space of transferable adversarial examples. *arXiv preprint arXiv:1704.03453*, 2017.
- [24] P. Warden. Speech commands: A dataset for limited-vocabulary speech recognition. *arXiv preprint arXiv:1804.03209*, 2018.
- [25] Y. Yu, W.-Y. Qu, N. Li, and Z. Guo. Open-category classification by adversarial sample generation. *International Joint Conference on Artificial Intelligence (IJCAI)*, 2017.

## Supplementary Material

### A Experimental Setting

#### A.1 Urban-Sound dataset

Like [20], we convert 3-seconds audio sounds to single channel image-like data with size  $128 \times 128$  by extracting log-scaled mel-spectrograms with 128 bands, using a window size of 23 ms (1024 samples at 44100Hz) with the same stride size. If a given audio is more than 3 seconds long, we randomly clip a 3 second from its corresponding mel-spectrogram patch and if it is less than 3 seconds, its patch is padded to make all it 128. furthermore, we consider the CNN described in Table 4 trained for 150 epochs using SGD with learning rate of 0.001 with momentum 0.9.

To train A-CNN for Urban-Sound on ECS (as an OOD set), we remove the overlap classes between ECS and Urban-Sound.

L#1	Conv: [1, 24, 5, 1, 2]; maxpool: [4, 2, 0]; relu
L#2	Conv: [24, 48, 5, 1, 2]; maxpool: [4, 2, 0]; relu
L#3	Conv: [48, 48, 5, 1, 2]; maxpool: [4, 2, 0]; relu
L#4	Conv :[48, 128, 5, 1, 2]; maxpool: [4, 2, 0] ;relu
L#5	Fully Connected (FC): [4608, 128]; dropout: 0.5; relu
L#6	FC layer : [128, 10]; softmax

Table 4: CNN used for Urban-Sound dataset. Conv: [#input channels, #out channels, kernel size, stride, padding], maxpool: [kernel size, stride, padding] and FC: [ input dim, output dim]

#### A.2 Hyper-parameters of threshold-based detectors

Using two validation sets one involving in-distribution samples and another consists of OOD samples from an OOD set, we tune hyper-parameters of ODIN and Mahalanobis detector for achieving their best results on the validation sets. For ODIN, we consider magnitude noise from  $\{0.0, 0.0005, 0.0014, 0.001, 0.01\}$  and temperature set to 1000 for all experiments. For Mahalanobis-detector, magnitude of noise tuned from  $\{0.0, 0.005, 0.002, 0.0014, 0.001, 0.0005\}$ .

### B Results Details

We report in Table 5, the numeric values of our metrics computed for OOD sets of in-distribution sets as well as our metric values for *test in-distribution sets*. Although the latter set (in-distribution test sets) are not at all OOD, we just show their behaviour for covering their own sub-manifolds, which are approximated by *in-distribution training samples in the feature space*. As expected, in-distribution test sets have the largest coverage ratio and SE as well as the smallest CD since they actually belong to their corresponding manifolds, where they are supposed to exactly lie.

In Table 6, TNR or rejection rate of OOD sets achieved by various state-of-the-art methods and A-CNN\* are presented.

#### B.1 Black-box Fast Gradient Sign (FGS) Adversaries

FGS adversaries with high noise level can be regarded as synthetic OOD samples. Even though such FGS adversaries contain perceptible noise, i.e., noticeable by human eyes, they can still fool vanilla CNNs easily [8, 23]. To explore the capability of A-CNN\* in detecting such non-optimal adversaries, A-CNN\*, A-CNN‡, and their vanilla counterparts are compared w.r.t. their error rates on FGS adversaries with varying amount of noise. We generated 5,000 black-box FGS adversaries (from training in-distribution set) using another pre-trained vanilla CNN (different from the one evaluated here). Some samples are displayed in Table 3.

As evident from Fig 2, error rates (i.e., 1-Acc) of vanilla CNNs increase as  $\alpha$  becomes larger, showing the transferability of these black-box FGS adversaries. In contrast, the error rates (i.e., 1-(Acc+Rej)) of the A-CNNs\* approach zero (Fig 2) as  $\alpha$  increases since many of these FGS samples are rejected by A-CNNs\*. Fig 2 (b) and (d) can explain this phenomenon; larger  $\alpha$  causes generated FGS adversaries to be further away from the sub-manifolds of in-distribution classes (i.e., larger CD). When FGS

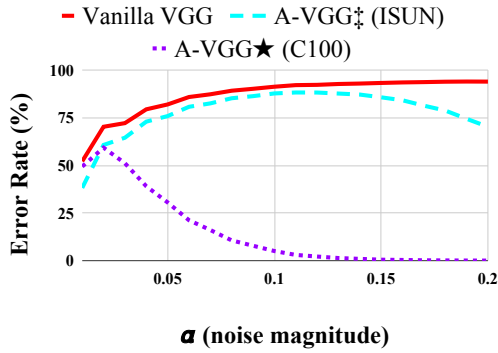
In-dist.	OOD sets	CR (%) $\uparrow$	SE $\uparrow$	CD $\downarrow$
SVHN	Gaussian	14.91	2.035	2.13
	LSUN	14.63	2.054	2.16
	C100	15.66	2.181	2.17
	T-ImgNt	13.83	2.109	2.21
	C10	14.39	2.11	2.23
	ISUN	11.37	2.073	2.3
	Test in-dist	<b>70.67</b>	<b>2.302</b>	<b>0.55</b>
C10	Gaussian	1.93	0.264	2.23
	SVHN	9.04	1.538	2.39
	C100*	21.39	2.158	2.49
	T-ImgNt	16.46	1.908	2.68
	ISUN	13.28	1.766	2.68
	LSUN	12.93	2.039	2.95
	Test in-dist	<b>80.98</b>	<b>2.3</b>	<b>1.034</b>
Audio	WhiteNoise	1.110	0.031	0.87
	command	27.08	0.654	0.32
	ECS	40.62	2.093	0.44
	TuT	15.79	1.382	0.048
	Test in-dist	<b>28.70</b>	<b>2.21</b>	<b>0.36</b>

Table 5: Numeric values of our proposed metrics for OO sets and in-distribution test set.

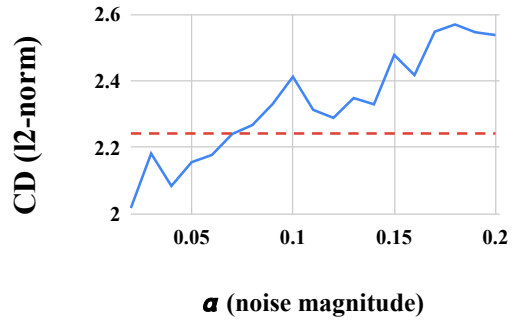
In-distribution Task	OOD sets	OOD Rej. rate (TNR) $\uparrow$			
		Baseline	ODIN	Mahalanobis	Augmented CNN*
SVHN	C100	58.08	67.91	94.66	99.82
	LSUN	54.84	67.57	99.73	100
	ISUN	62	73.45	100	99.86
	T-ImageNet	58.7	70.22	99.37	99.99
	C10	56.73	67.48	93.26	99.75
	AVG	58.07	69.326	97.404	99.88
	C10	C100*	35.52	45.94	42.73
LSUN		48.96	74.04	98.7	91.03
ISUN		45.83	68.75	91.76	70.08
T-ImageNet		45.85	66.88	96.4	90.7
SVHN		47.83	73.02	73.79	87.26
AVG		44.8	65.726	80.676	85.1
Urban-sound	Command	12.47	19.47	20.34	35.26
	ECS	35.99	35.19	33.63	86.85
	TuT	74.40	87.66	82.29	44.1
	AVG	40.95	47.44	45.42	55.40

Table 6: Rejection rates (TNR) of OOD sets by state-of-the-art approaches and A-CNN\* .

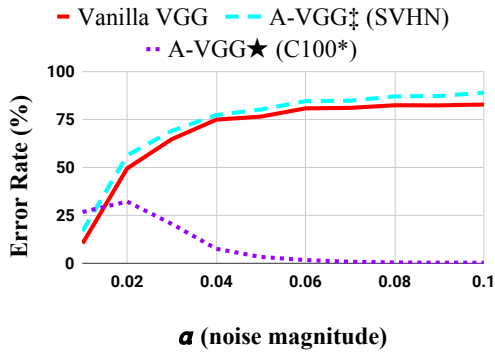
adversaries enter the protected regions by A-CNN\* (starting at the distance denoted by CD of the most protective OOD set, i.e., dotted red horizontal line), they are automatically rejected as OOD samples.



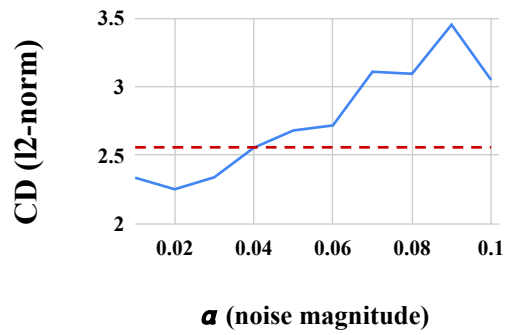
(a) Rejection rate of SVHN FGS adversaries



(b) CD of SVHN FGS adversaries



(c) Rejection rate of CIFAR-10 adversaries



(d) CD of CIFAR-10 adversaries

Figure 2: FGS adversaries with various noise magnitude. Sub-figures (a,c) show error rates of vanilla CNN, A-CNN<sup>\*</sup>, A-CNN<sup>†</sup> on FGS adversaries with varying noise for SVHN and CIFAR-10, respectively. Note Err rate = 1-(Acc rate +Rej rate). (b,d) Coverage Distance (CD) of FGS adversaries (their average distance to in-distribution sub-manifolds) for SVHN and CIFAR-10 respectively. The dotted red line is the Coverage Distance of the most protective OOD set, which is used to train A-CNN<sup>\*</sup>.

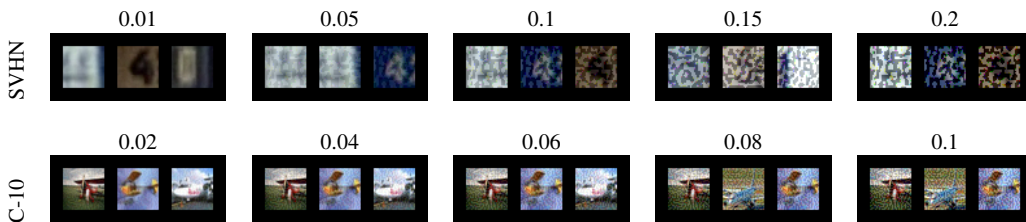


Figure 3: FGS adversaries for SVHN and CIFAR-10 with various amount of noise, magnitude of noise (i.e.  $\alpha$ ) shown on top of each sub-figures.